ISIJ International, Vol. 43 (2003), No. 12, pp. 1983–1988

Oxidation Behavior of High-speed Steels in Dry and Wet Atmospheres

Hyung-Hwan KIM, Ju-Wan LIM[1)] and Jung-Joong LEE[1)]

Hynix Semiconductor Inc., San 136-1, Amiri, Bubal-eup, Ichon, Kyounggi-do 467-866, Korea.
1) School of Materials Science and Engineering, Seoul National University, San 56-1, Shinrim-dong, Kwanak-ku, Seoul 151-744, Korea.

(*Received on February 24, 2003; accepted in final form on July 2, 2003*)

The oxidation behavior of high-speed steel (HSS), which is used as the work rolls in hot strip mills, was examined under both wet and dry oxidation conditions. In a dry atmosphere, carbides as well as the martensite matrix were oxidized, while only the matrix was oxidized in the wet atmosphere. After dry oxidation, the M_2C-, M_6C- and M_7C_3-type carbides maintained their original shapes, while the MC-type carbides were oxidized into parallelepiped (orthorhombic) crystals. The parallelepiped oxides were easily removed from the sample surface due to their low adhesion strength. Double-layered oxides were formed after oxidizing the matrix, in dry as well as wet atmospheres. The outer layer showed a dense structure after dry oxidation, while a columnar and porous layer was formed in the wet atmosphere. In the early stages of oxidation, the high-speed steels oxidized following the parabolic rate law in both the dry and wet atmospheres. The parabolic weight change transformed to a linear one, when the oxide thickness was $>1.3\,\mu$m by dry oxidation. The transition to a linear weight change was not observed in the wet oxidation. It is believed that, in a dry atmosphere, cracks occurred due to stress accumulation in the oxide layer, while the porous oxide layer hindered crack formation during wet oxidation.

KEY WORDS: oxidation; high speed steel; carbides; double-layer oxide.

1. Introduction

Recently, the demand for rolling mills with improved mechanical properties, such as wear resistance, toughness and resistance to surface roughening, has increased considerably along with the demand to produce rolled products with higher qualities.[1)] Compound type rolls have been developed in order to meet these requirements. The outer part of the roll is made from high-speed steels (HSS) with a high hardness and wear resistance at high temperatures, while forged steel with a high toughness is used for the core part in order to avoid breakage in the case of high bending loads.[2,3)] Since the quality of the rolled products is closely related to the surface condition of the rolls,[4,5)] investigating surface deterioration is important for the development of the roll. It is known that the roll surface deteriorates due to thermal fatigue, abrasion, *etc.*[6)] The roll surface is easily oxidized as a result of the hot rolling processes, where the rolls are heated up to 600°C. Consequently, delamination of the oxidized layer is another important factor for surface deterioration. A complex oxidation behavior is expected because HSS contains many alloying elements and their carbides. Therefore, it is essential to study the oxidation behavior of HSS not only in a dry atmosphere but also in a wet atmosphere, as the roll is cooled with water during the rolling processes.

2. Experimental Procedures

The HSS samples were made from three different commercial rolls. **Table 1** shows the chemical compositions of the samples. Sample A has more W and Mo, and sample C has more Cr compared to the other. The samples were mechanically polished with SiC paper up to a grit number of 2 000, and ultrasonically cleaned in acetone and ethyl alcohol. For dry oxidation, the samples were heated to 600°C in a vacuum, and oxygen was introduced until the pressure in the oxidation chamber reached 1 atm. The samples were re-

Table 1. Compositions (wt%) of the HSS rolls investigated in this work.

	C	W	Mo	Cr	V	Si	Mn	P	S	Ni	Al
A	2.04	6.48	4.13	5.58	4.28	0.21	0.91	0.013	0.012	1.44	0.009
B	1.96	2.90	1.05	5.55	5.05	0.75	0.9	0.04	0.01	1.45	0.02
C	1.98	1.9	2.9	9.4	3.6	0.80	0.40	0.02	0.01		

Table 2. Dependence of the vapor pressure and flow rate of H_2O on the bubbler temperature.

Temperature of bubbler (℃)	50	65	82	92	97
Vapor pressure of H_2O(atm)	0.12	0.25	0.51	0.75	0.90
Flow rate of H_2O(sccm)	96	200	408	600	720

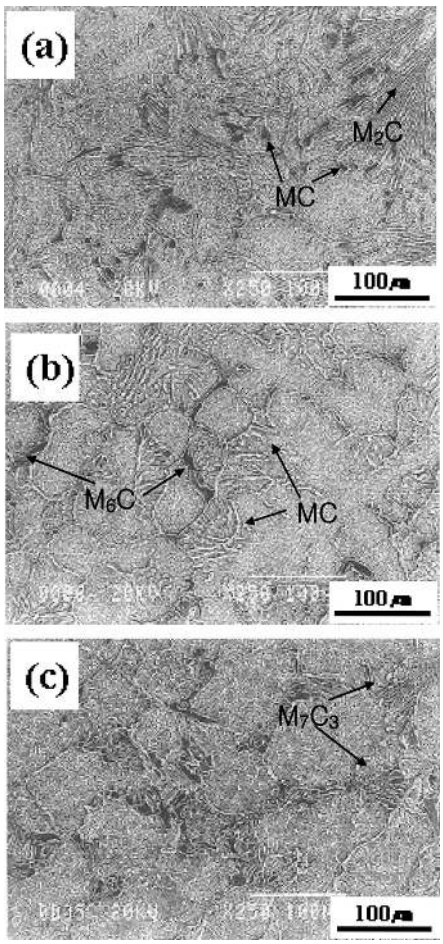

Fig. 1. Surface morphologies of the etched HSS: (a) specimen A, (b) specimen B, (c) specimen C.

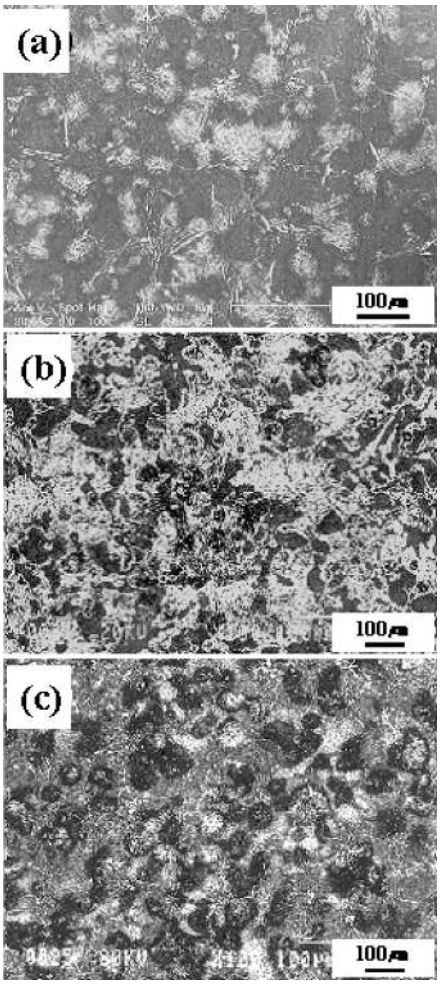

Fig. 2. SEM micrographs of the HSS oxidized in O_2: (a) specimen A, (b) specimen B, (c) specimen C.

moved from the chamber after oxidation for 5, 15, 30 and 60 min. The wet atmosphere was obtained by passing Ar gas through a distilled water bubbler. The humidity in the Ar was controlled by changing the bubbler temperature. The vapor pressure and flow rate of H_2O at different bubbler temperatures are shown in **Table 2**. X-ray diffraction (XRD), scanning electron microscopy (SEM), energy dispersive spectroscopy (EDS), and Auger electron spectroscopy (AES) were used to investigate the structure and composition of the oxidized specimens. Before the microstructural analysis, the specimens were etched in a solution of 30% hydrogen peroxide (100 mL) and 42% hydrofluoric acid (5 mL).[7] The isothermal oxidation behavior was studied using a Cahn thermo-gravimetric electro-balance during the dry oxidation. The thickness of each scale layer was measured to determine the oxidation rates during the wet oxidation experiment.

3. Results and Discussion

3.1. Structure of HSS Specimens

Figure 1 shows the surface morphologies of the three HSS specimens before oxidation. The carbides are located not only in the grain but also at the grain boundary. Different types of carbides are known to exist in HSS. However, it was not easy to classify the carbides by only the XRD peaks. As the carbides have different shapes and components, they could be better identified by observing the etched samples by SEM[7,8] and by EDS analysis. In specimen A, feather-shaped M_2C-type carbides and MC-type carbides in the form of small black particles can be seen, while specimen B shows M_6C-type carbides and coral-shaped MC-type carbides. In specimen C, the M_7C_3-type carbides, which contain more Cr than the other carbides appeared. Fine secondary MC carbides precipitated in the cells of all samples.

3.2. Oxidation in a Dry Atmosphere

Figure 2 shows the surface morphology of the specimens after oxidation for 5 min. All carbides except MC were oxidized maintaining their original shapes. **Figure 3** shows the oxides of the martensite matrix, MC- as well as M_2C-carbides. The whisker type oxides can be observed on the ma-

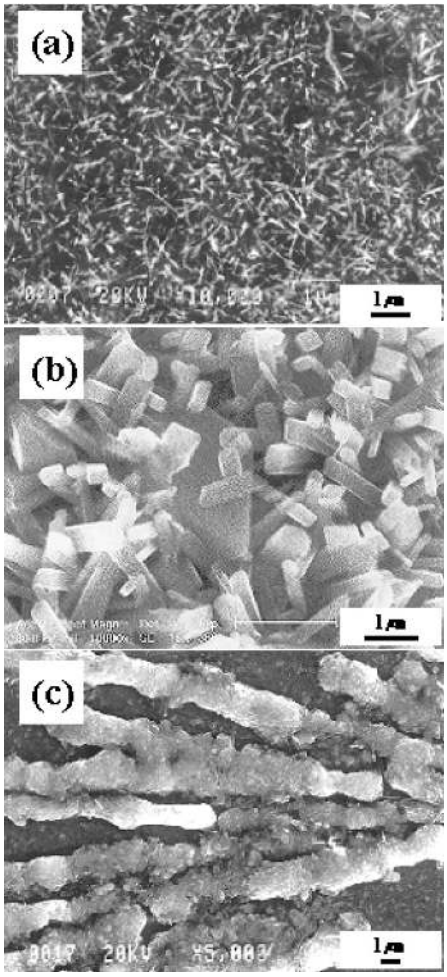

Fig. 3. Different morphologies in the oxidized HSS: (a) Fe matrix, (b) MC carbide, (c) M_2C carbide.

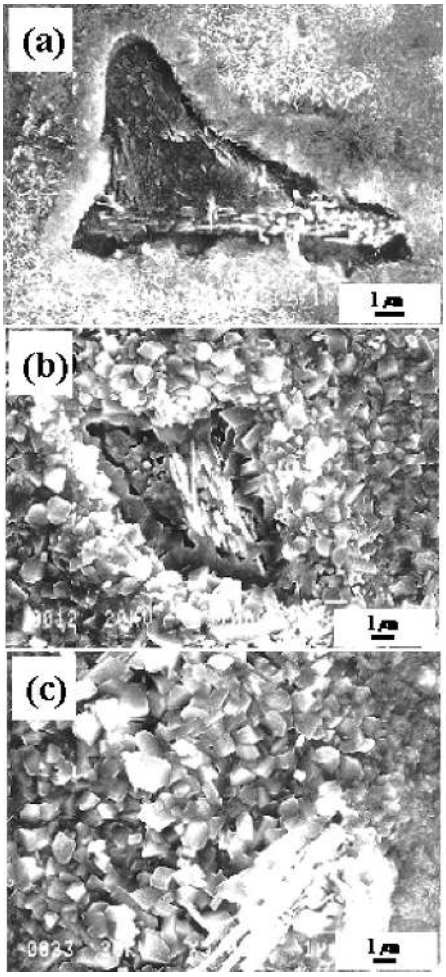

Fig. 5. Oxidation of the MC carbide in O_2 with time (specimen B): (a) 5 min, (b) 15 min, (c) 30 min.

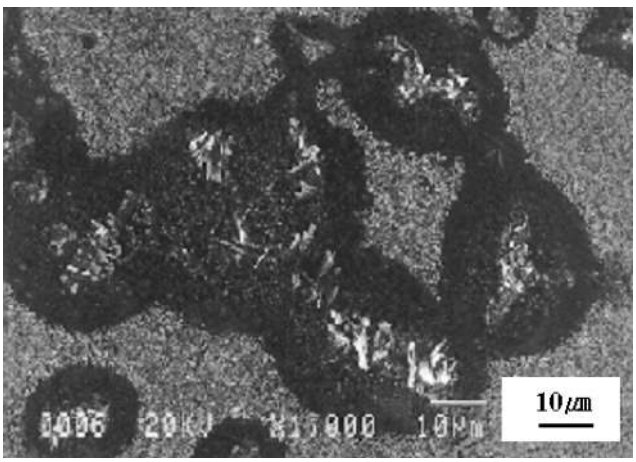

Fig. 4. Surface morphology of the HSS around the MC carbides.

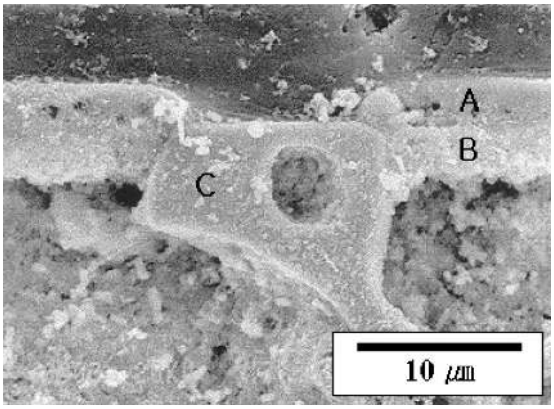

Fig. 6. Cross-sectional morphology of the HSS oxidized in O_2.

trix surface, which indicates that the oxidation reaction was a diffusion-controlled process.[9] All carbides oxidized faster than the matrix, and the oxides grew higher over the oxidized surface of the matrix. The MC-carbides oxidized forming parallelepiped crystals with a length of 3–5 μm. EDS and XRD analyses showed that the black area around the oxides of the MC-carbides (**Fig. 4**) was a vanadium rich iron oxide. The area became larger and transformed into parallelepiped crystals as oxidation proceeded (**Fig. 5**). **Figure 6** shows the cross-sectional view of an oxidized sample. The unoxidized matrix was removed by etching to observe the oxidized structure more clearly. It was found that the two oxide layers were formed after oxidizing the matrix. The outer layer was composed of Fe_2O_3 and Fe_3O_4, while the inner one was identified as Fe_3O_4 by XRD analysis (**Fig. 7**). The outer layer was formed by the outward diffusion of Fe ions from the matrix, while the inner one was formed by the inward diffusion of oxygen ions. This can be deduced from the fact that the carbides could be found only in the inner layer. The parallelepiped oxides on the MC-carbide were easily removed by the sample preparation, which

indicates a very low adhesion strength of the oxides. The oxides did not form a protective layer so that oxygen could be transported easily through the oxides to the surface of the non-oxidized carbides.

The results from the isothermal oxidation experiments are shown in **Fig. 8**. All specimens oxidized following the parabolic rate law in the early stage. However, for specimens A and B, the parabolic weight change transformed to a linear one when the weight increased by approximately 0.2 mg/cm^2, which corresponds to the oxide thickness of 1.3 μm. When the thickness of the oxide layer increased, the stress in the layer also increased until cracks were produced in the layer.[10–12] It is supposed that the enhanced weight increase is due to the oxidation by gaseous oxygen, which is transported through the cracks. Specimen C, on the other hand, contained much more Cr (see Table 1), and the oxidation rate was lower due to the formation of a protective Cr rich oxide on the surface.[13] The oxide thickness of specimen C did not reach the critical value, and the sample did not show any deviation from the parabolic rate curve.

3.3. Oxidation in a Wet Atmosphere

Figure 9 shows the surface morphology of the specimens before and after 30 min of wet oxidation. Carbides were not oxidized during the oxidation of the matrix. Therefore, the original shape remained after the oxidation. The AES depth profile (**Fig. 10**) confirms that the carbides did not oxidize in a wet atmosphere. It is assumed that in a wet atmosphere the vapor pressure of oxygen was not high enough to oxidize the compounds. A double oxide layer was also formed as in the case of dry oxidation (**Fig. 11**).

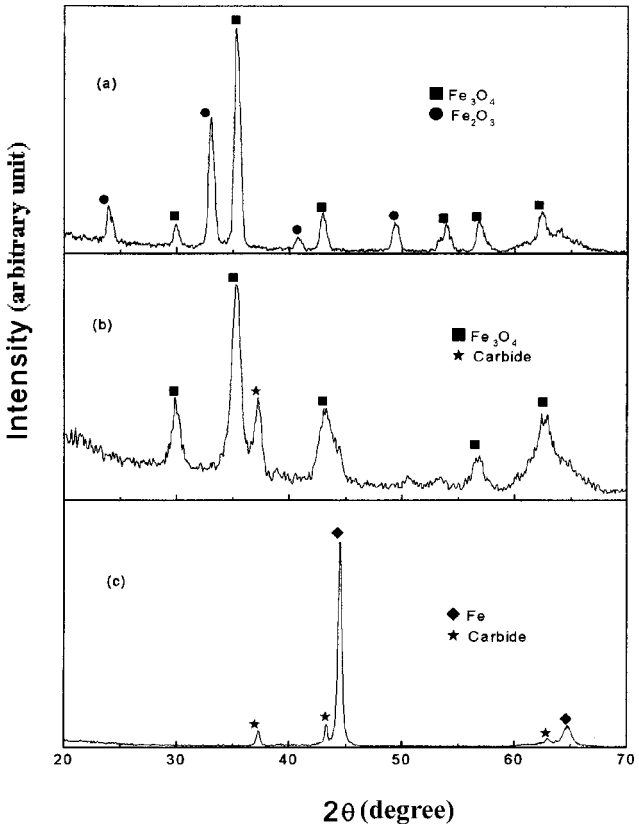

Fig. 7. XRD patterns of the oxidized HSS (specimen B): (a) after oxidation, (b) after outer layer removed, (c) before oxidation.

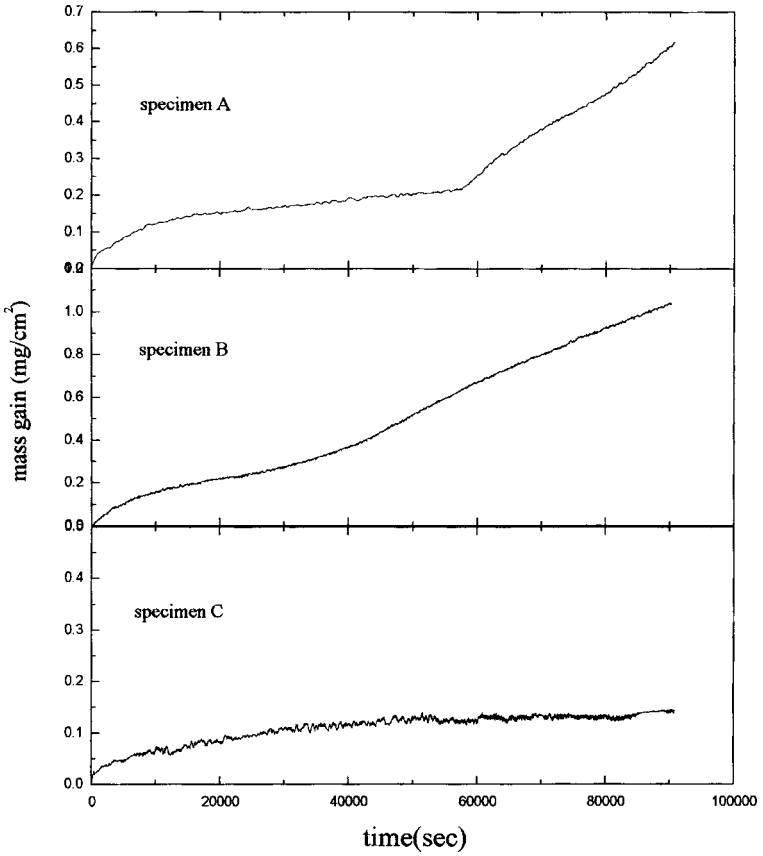

Fig. 8. Overall stage in Mass gain of HSS by oxidation in O_2 at 600°C.

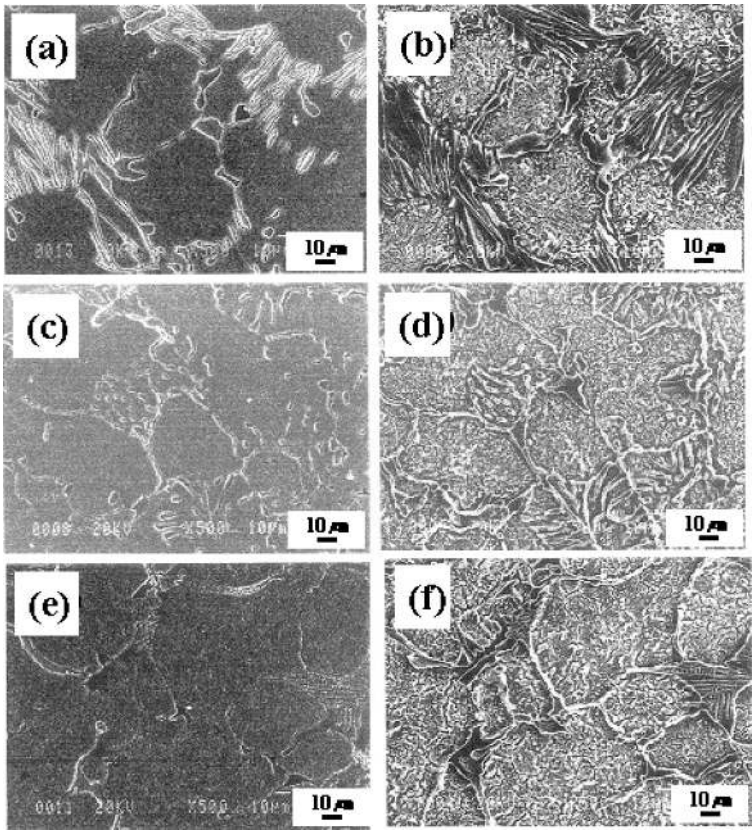

Fig. 9. Surface morphologies of an oxidized specimen and etched specimen: (a) oxidized specimen A, (b) etched specimen A, (c) oxidized specimen B, (d) etched specimen B, (e) oxidized specimen C, (f) etched specimen C (p_{H_2O}=0.90 atm).

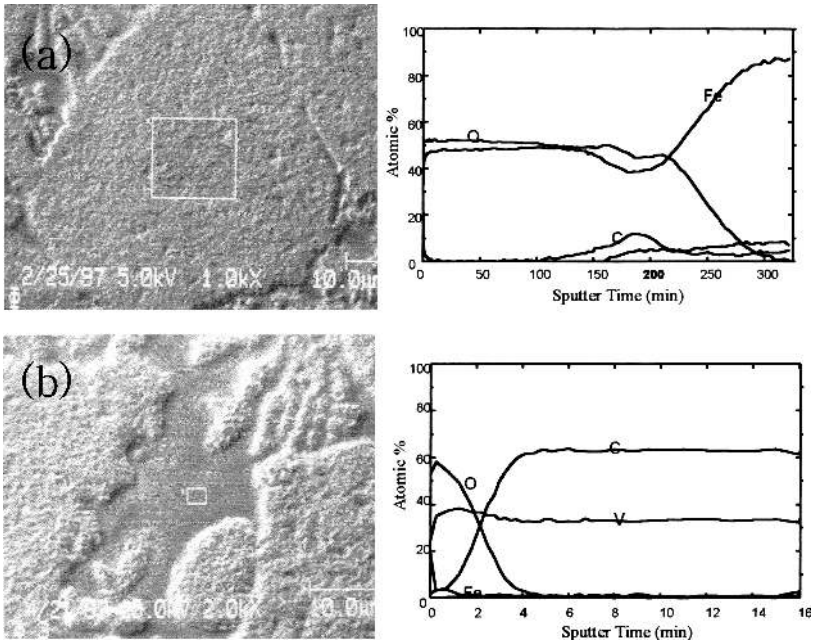

Fig. 10. AES depth-concentration profile of oxidized HSS (specimen B, 30 min): (a) matrix, (b) carbide.

The outer layer was formed with a columnar and porous structure, while the inner one showed a fine and dense microstructure. The defects in the outer layer accelerated oxygen- and Fe-ion diffusion. Therefore, the oxide layer was thicker than that produced by dry oxidation. The results from the isothermal oxidation (**Fig. 12**) show that all specimens oxidized following the parabolic rate law as in the case of dry oxidation. The oxidation rate of specimen C with the higher Cr content was also lower than that of the other specimens due to the formation of a protective Cr-rich oxide layer.[13] However, a transition to a linear weight change was not observed under the wet oxidation conditions. It is assumed that defects in the outer layer released the stress and prevented the crack formation in the oxide

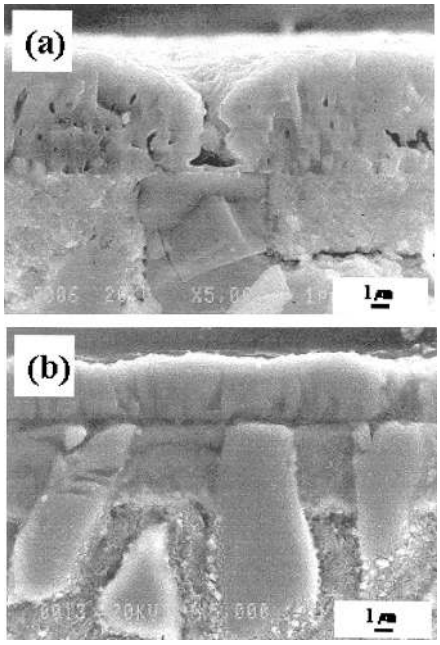

Fig. 11. Cross-sectional image of HSS around the carbide (specimen B): (a) fractured image, (b) etched image (p_{H_2O}= 0.90 atm).

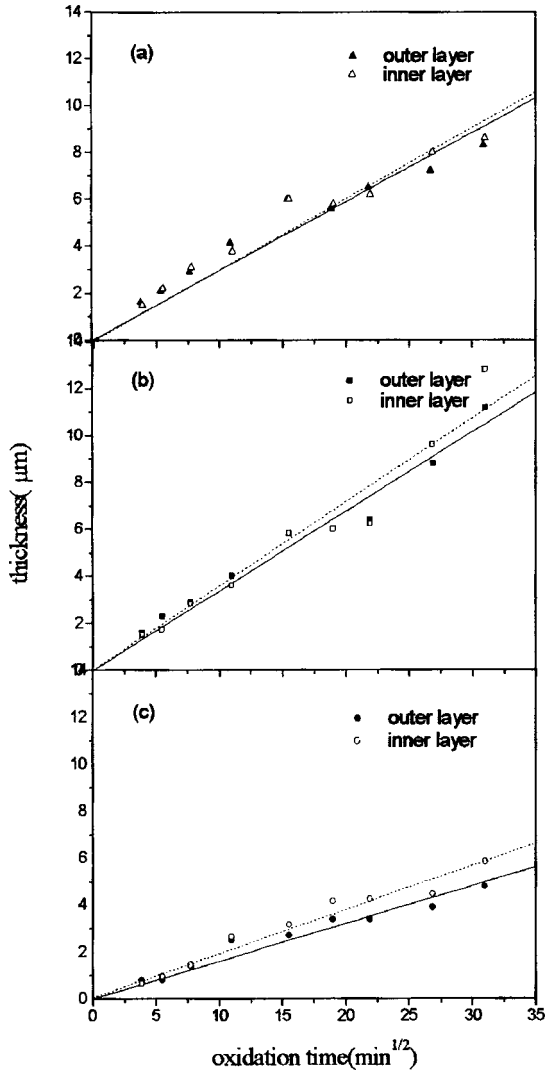

Fig. 12. Oxidation rates of HSS in the wet atmosphere at 600°C: (a) specimen A, (b) specimen B, (c) specimen C.

layer.[10–12]

4. Conclusion

The oxidation behavior of high-speed steels with different concentrations of alloying elements was investigated in a dry as well as a wet atmosphere.

(1) Carbides as well as the matrix were oxidized in a dry atmosphere, while in a wet atmosphere only the matrix was oxidized.

(2) When the carbides were oxidized in a dry atmosphere, the M_2C-, M_6C- and M_7C_3-type carbides maintained their original shapes, while the MC-type carbides oxidized into parallelepiped crystals.

The adhesion strength between the oxides and the unoxidized MC-type carbides was very small, and the oxides could be removed easily from the surface.

(3) A double-layered oxide was formed after oxidizing the matrix in the dry as well as wet atmospheres. The outer layer was formed by the outward diffusion of Fe ions from the matrix, which was composed of Fe_2O_3 and Fe_3O_4 in both cases. In the dry atmosphere, a dense outer layer was formed, while in the wet atmosphere, the layer was porous and had a columnar structure. The inner oxide layer was composed of Fe_3O_4 in both cases.

(4) In the dry as well as wet atmospheres, the high-speed steels oxidized following the parabolic rate law in the early stage. However, in the dry atmosphere, the parabolic weight change transformed to a linear one, when the oxide thickness increased up to approximately 1.3 μm, due to crack formation in the oxide layer. In the wet atmosphere, the transformation to a linear weight change was not observed.

Acknowledgement

The authors are grateful for the financial support provided by the Korea Science and Engineering Foundation through the Center for Advanced Plasma Surface Technology at the Sungkyunkwan University (2003).

REFERENCE

1) M. Hashimoto, S. Otomo, R. Kurahashi and T. Kouga: *ISIJ Int.*, **32** (1992), 1202.
2) M. Shimizu, O. Shitamura, S. Matsuo, T. Kamata and Y. Kondo: *ISIJ Int.*, **32** (1992), 1244.
3) Y. Sano, T. Hattori and M. Haga: *ISIJ Int.*, **32** (1992), 1194.
4) Y. Oike, K. Yoshitake and S. Yamanaka: *ISIJ Int.*, **32** (1992), 1211.
5) J. H. Ryu, O. J. Kwon, P. J. Lee and Y. M. Kim: *ISIJ Int.*, **32** (1992), 1221.
6) O. Kato, H. Yamamoto M. Ataka and K. Nakajima: *ISIJ Int.*, **32** (1992), 1216.
7) P. Ding, G. Shi and S. Zhou: *Mater. Charact.*, **29** (1992), 15.
8) Y. Matsubara: *J. Korean Foundrymen's Soc.*, **17** (1997), 16.
9) S. C. Choi, H. J. Cho, Y. J. Kim and D. B. Lee: *Oxid. Met.*, **46** (1996), 51.
10) H. E. Evans: *Int. Mater. Rev.*, **40** (1995), 1.
11) M. Schütze: Protective Oxide Scales and Their Breakdown, Wiley, New York, (1997), 67.
12) J. E. Castle: Corrosion, Vol. 1, 2nd ed., Newnes-Butterworths, Sevenoaks, Kent, (1976), 1: 241.
13) F. H. Stott, G. C. Wood and J. Stringer: *Oxid. Met.*, **44** (1995), 113.
14) J. E. Castle and H. G. Masterson: *Corros. Sci.*, **6** (1966), 93.
15) P. Kofstad: *Oxid. Met.*, **24** (1985), 265.